

# CHARACTERISATION OF MICROCRACKS AND THEIR INFLUENCE ON TRANSPORT PROPERTIES OF CEMENTITIOUS MATERIALS

Z. Wu, M.J. Mac, H.S. Wong, N.R. Buenfeld

Concrete Durability Group, Imperial College London, UK.

## Introduction

Microcracks are known to form in concrete when subjected to drying and it has long been suspected that they could impact transport properties and durability of concrete structures. However, very few studies have been carried out to thoroughly characterise the microcracks or correlate their characteristics to transport. More crucially, no attempts have been made to isolate the influence of microcracks from other factors (e.g., water content, pore structure). Thus, it has not been conclusively shown whether microcracks impact transport properties and to what extent. This project aims to enhance our understanding of microcracks by: a) developing 2D & 3D imaging techniques to characterise microcracks; b) quantifying the effect of microcracks on transport; c) investigating factors influencing microcrack formation; and d) providing experimental data for modelling of transport processes in microcracked concrete. This paper presents some of the findings to date from on-going experiments and discusses challenges and future work.

## Methodology

Concrete, mortar and paste specimens were prepared with CEM I 32.5 R at w/c 0.35 and 0.50, then sealed cured for 3, 28 and 90 days. Limestone (<10 mm) and siliceous sand (< 5mm) were used as coarse and fine aggregate respectively. Total aggregate content was 68% vol. After curing, samples were conditioned to equilibrium by drying at 105°C, 50°C or 21°C at 35% RH or by 'gentle' stepwise drying from 93% RH to 86%, 75%, 66%, 52%, 35% and 3% RH at 21°C. Several drying regimes were used to produce varying degrees of microcracking. Oxygen diffusivity, oxygen permeability, sorptivity and electrical conductivity were measured on disc samples (100Ø × 50 mm) in three replicates. Microcracks were characterized using fluorescence microscopy (FM) and image analysis. Disc samples were pressure-impregnated (7 bars) with fluorescein-dyed epoxy. An 8mm thick slice was sectioned from the centre of each disc and imaged with a petrographic microscope in fluorescence mode. A series of overlapping images was captured at 50x magnification (2048×1536, pixel size 0.9µm) and stitched to give a high-resolution montage of the entire sample. Characteristics of the observed microcracks such as number of cracks, width, length, density and orientation with respect to drying surface were quantified with image analysis. Selected samples were also characterised using backscattered electron microscopy (BSE), 3D laser scanning confocal microscopy (LSCM) and X-ray computed tomography (µ-CT).

## Microcracks induced by drying

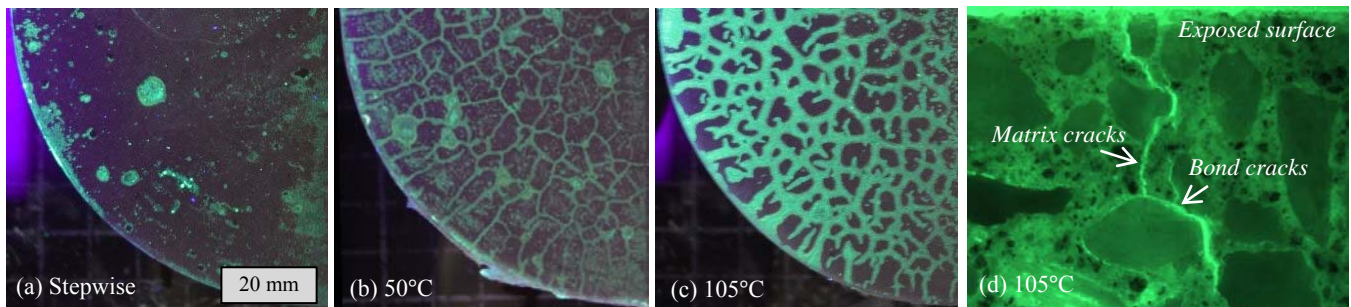


Fig. 1 Microcracking on the exposed surface of pastes (a-c) and interior of concrete (d) induced by drying.

Fig. 1 shows typical microcracking seen on paste and concrete. Severely dried samples tend to show a characteristic map-cracking on the exposed surface caused by volume changes that is restrained either by underlying materials or aggregate particles. Stepwise drying produces a relatively small moisture gradient within the specimen so the amount of microcracking reduced significantly. The detectable microcracks are concentrated near the surface region, have widths ranging from 1 to 60 microns and extend to depths of several mm into the sample. The average crack widths and orientation measured on the cross-section of 3-day cured concretes subjected to different drying regimes are shown in Table 1. The total number of microcracks measured per sample ranged between 241 and 702. Microcrack densities were 0.252, 0.177, 0.145 and 0.05 mm<sup>-1</sup> for concretes dried at 105°C, 50°C, 35% RH and stepwise respectively. The results show that increasing the severity of drying produces more microcracking, and increases the widths and

lengths of the microcracks. The orientation is influenced by the presence of aggregates (Fig. 1d), but on average is almost perpendicular to the exposed surface (Table 1). This indicates that the microcracks are indeed induced by the drying treatment. We have also found that mortars have less microcracking, lower crack widths and crack density compared to similar concretes (w/c ratio, age, aggregate content), in agreement with [1].

Table 1 Average widths and orientation of microcracks measured on cross-section of concrete samples. Standard errors are shown in brackets.

w/c	Average width ( $\mu\text{m}$ )				Orientation with respect to drying surface ( $^\circ$ )			
	105°C	50°C	35%RH	Stepwise	105°C	50°C	35%RH	Stepwise
0.50	8.8 (0.10)	7.6 (0.45)	5.6 (0.35)	4.2 (0.16)	88.5 (2.2)	84.6 (3.7)	87.0 (3.3)	86.1 (2.7)
0.35	9.8 (0.15)	6.6 (0.50)	4.1 (0.30)	3.0 (0.30)	87.2 (3.0)	90.9 (3.5)	89.4 (2.8)	95.1 (7.7)

### Transport properties

Measurements show that increasing the severity of drying increases the measured oxygen diffusivity and permeability significantly. For example, the data in Table 2 for 3-day cured concrete show that diffusivity increased by a factor of 3.4-5.1 while permeability increased by a factor of 4.2-5.7 when comparing stepwise drying to oven drying at 105°C. The increase in transport is more significant in samples that are less porous (lower w/c ratio). One may be tempted to attribute the increase in transport to the influence of microcracks, but this is not as straightforward as it seems because the change in moisture content would also make a significant contribution. Removing more moisture increases the accessible porosity and this effect is compounded by microcracks that develop with drying. Whether or not the influence of microcracks can be isolated remains a question. On-going tests on sorptivity, electrical conductivity and chloride penetration of re-saturated samples may shed further insights into this issue.

Table 2 Transport properties of 3-day cured concrete after drying. Standard errors are shown in brackets.

w/c	$\text{O}_2$ diffusivity ( $\times 10^{-8} \text{ m}^2/\text{s}$ )				$\text{O}_2$ permeability ( $\times 10^{-17} \text{ m}^2$ )			
	105°C	50°C	35%RH	Stepwise	105°C	50°C	35%RH	Stepwise
0.50	18.8 (0.11)	15.5 (0.40)	9.97 (0.72)	5.49 (0.25)	33.1 (1.04)	20.3 (0.85)	12.8 (1.04)	7.87 (0.46)
0.35	14.1 (0.15)	11.7 (0.14)	5.99 (0.77)	2.76 (0.26)	10.7 (0.56)	8.05 (0.39)	2.98 (0.56)	1.84 (0.23)

### Influence of confining pressure on transport properties

Perhaps one method to study the influence of microcracking in isolation is to measure transport properties while the sample is subjected to increasing confining pressure. Fig. 2 shows the diffusivity and permeability of concrete (w/c 0.5, 3 & 28 day cured) obtained at confining pressures of 0.3, 0.6, 1.2 and 1.9 MPa. Error bars indicate +/- one standard error of the measurement and results are normalised to the value at 0.3MPa for each series. Further details of the experimental setup are given in [2]. Note that the lowest confining pressure was sufficient to seal the sample to prevent leakage around the curved face.

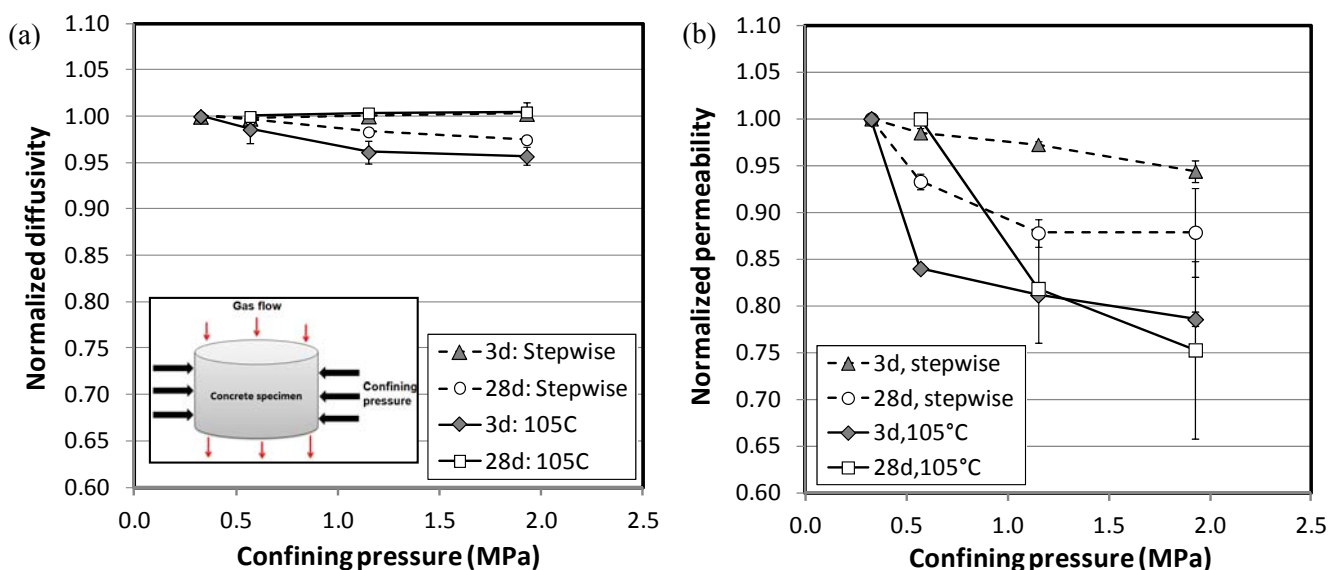


Fig. 2 Effect of confining pressure on (a) diffusivity and (b) permeability of 3d & 28d concrete (w/c 0.5).

The results show that increasing confining pressure can cause a drop in the measured transport property. This is more significant for permeability and for samples dried at 105°C regardless of curing age, suggesting that closure of microcracks occurs when the sample is confined. Because the microcracks are near perpendicular to the surface and propagate into the sample, their closure is expected to impact transport. Decrease in permeability is likely to continue beyond 2MPa. However, diffusion is less sensitive to the presence of microcracks and hence confining pressure. Most concrete structures in service are subjected to compressive stresses much higher than the largest confining pressure tested in this work. Thus, our results suggest that drying induced microcracks would not play a major role in transport of aggressive species in concrete under compression. In concrete subjected to tensile stresses however, the microcracks are likely to widen and propagate, and potentially accelerate the transport of aggressive species. Further work is necessary to better understand the influence of microcracks on the properties of concrete under load.

### Effect of rewetting on transport properties

Another approach to isolate the effects of microcracking and water content is to recondition samples (that were initially dried at 105°C, 50°C and 35%RH) at gradually increasing humidity so that they reach a similar moisture content as those subjected to step-wise drying. Transport properties are measured when the sample equilibrates at each RH step. This is an arduous process and has yet to complete after 18 months of testing. Results to-date (Fig. 3) show that transport is a strong function of water content, but the influence of microcracks is also evident. For example, at a water content of 0.8%, the permeability of the w/c 0.5 concrete dried at 105°C is 22% higher compared to the same concrete dried at 50°C. For diffusivity, the difference is about 11%. The residual difference in transport may be attributed to the additional microcracking that forms at 105°C compared to 50°C. However, some caution must be exercised in interpreting the data because when samples are rewetted: a) condensation may also occur in the microcracks, and b) further hydration may densify the pore structure or encourage crack healing. Thus, the contribution of microcracks to transport properties is likely to be underestimated via this approach. Furthermore, moisture hysteresis that occurs when a dried sample is reconditioned at higher humidity is another source of complication.

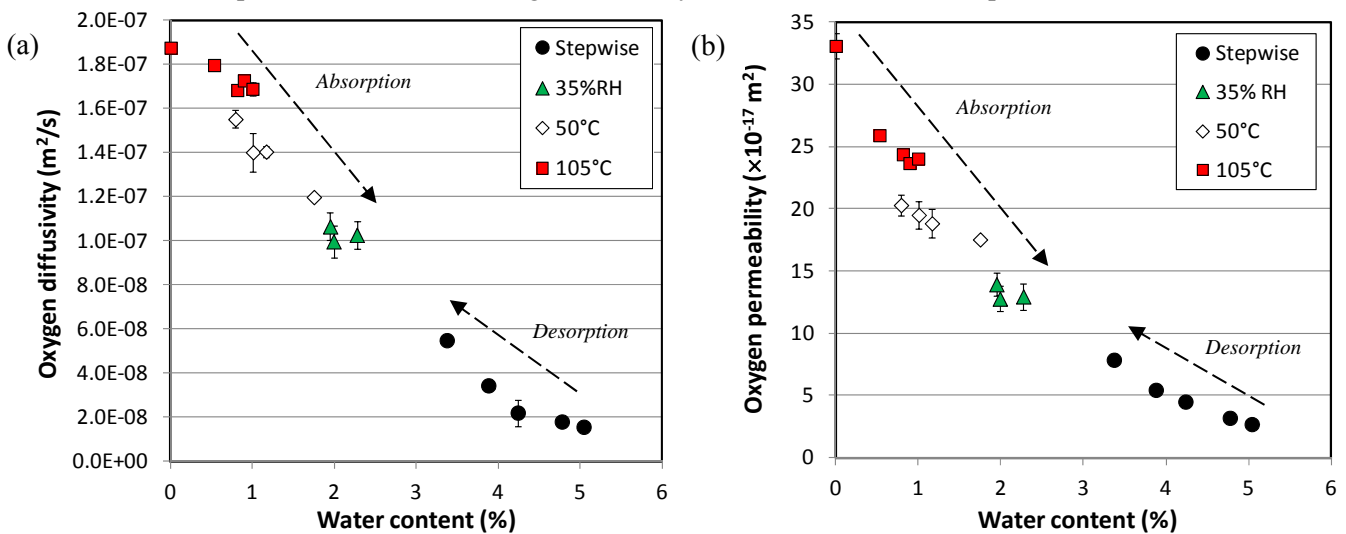


Fig.3 Effect of moisture content on a) diffusivity and b) permeability of concrete (w/c 0.5, 3d cured).

### Characterising microcracks in three-dimensions

We would like to image a representative volume of concrete in 3D and at sufficiently high resolution to capture the microcracks. This will help us understand how microcracks form and propagate. It will also improve our ability to model the influence of microcracks on transport (see companion paper) and to isolate other influencing factors. However, none of the existing imaging techniques that we have assessed to-date satisfy these criteria (Fig. 4). FIB-nt is capable of nano-scale resolution, but is practically limited to reconstruction of only a few microns thick sample.  $\mu$ -CT can image a large volume of concrete, but it only detects cracks wider than 10 $\mu$ m (Fig. 5). LSCM has a better resolution and can image a large area, but its imaging depth is limited to tens of microns (Fig. 6b). BSE and FM have very good resolution and are well-suited for large area imaging, but only in 2D. Perhaps the only way to fully characterise microcracks is to integrate information from several techniques. We are also exploring the potential of extending the imaging depth of LSCM substantially (while maintaining its resolution) by serial-sectioning and reconstructing the 3D stacks.

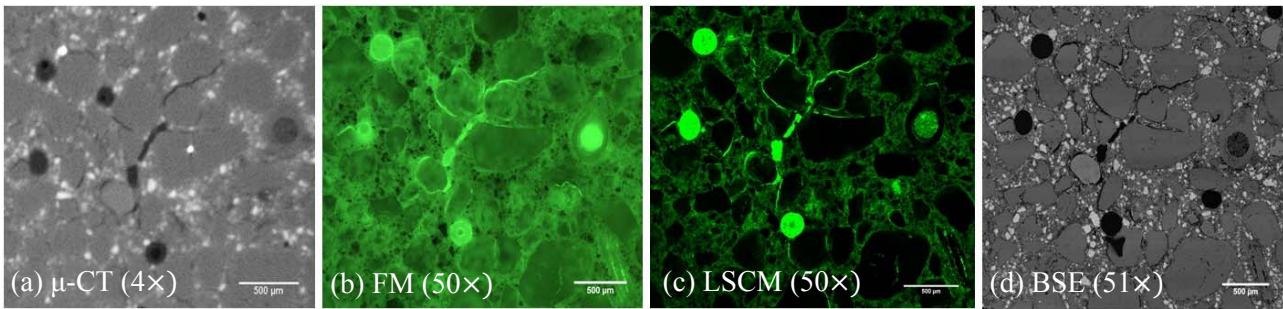


Fig. 4 Comparison of four techniques for imaging microcracks in concrete (w/c 0.5, 3d, 105 °C dried).

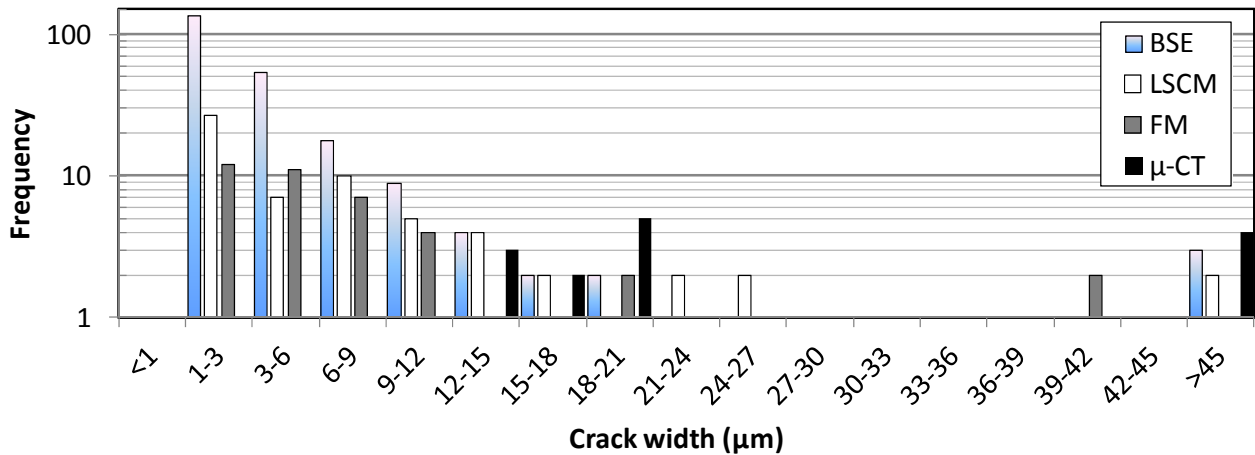


Fig. 5 Crack width distribution in concrete (w/c 0.5, 3d, 105 °C dried) measured by different methods.

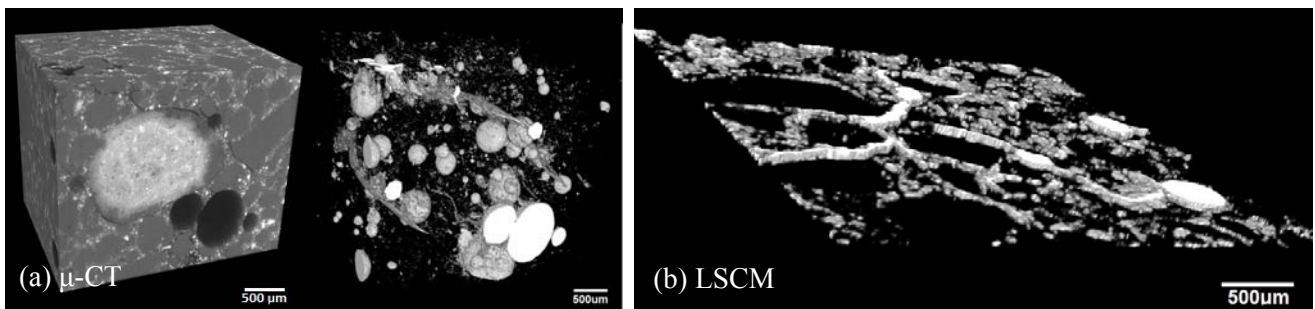


Fig. 6 3D reconstruction showing microcracks around aggregate particle using  $\mu$ -CT and LSCM

## Conclusions

Results from on-going experiments to characterise microcracks and their influence on transport properties were presented. Increasing the severity of drying has been found to increase the amount, widths and lengths of the microcracks, and the measured transport properties. However, applying a confining pressure decreases the measured transport, possibly due to closure of the microcracks. Future work will focus on decoupling the influence of moisture content, characterising the microcracks in 3D and using images of microcracks as input to model transport properties.

## ACKNOWLEDGEMENTS

The research leading to these results has received funding from the European Union Seventh Framework Programme (FP7 / 2007-2013) under grant agreement 264448.

## REFERENCES

- [1] H.S. Wong, M. Zobel, N.R. Buenfeld, R.W. Zimmerman, Influence of the interfacial transition zone and microcracking on the diffusivity, permeability and sorptivity of cement-based materials after drying, *Mag. Concr. Res.* 61 (2009) 571-589.
- [2] Z. Wu, H.S. Wong, N.R. Buenfeld, Effect of confining pressure on gaseous transport properties of concrete, *Cement & Concrete Science Conference*, Portsmouth, UK, 2-3 September, 2013.